Steady Metal Combustor as a Closed Thermal Energy Source

E. G. Groff* and G. M. Faeth†
The Pennsylvania State University, University Park, Pa.

A thermal energy source is described which can be used with closed thermodynamic cycles to obtain a power system that is independent of the environment. The energy source is based on the steady combustion of gaseous sulfur hexafluoride and liquid lithium, yielding liquid lithium fluoride and lithium sulfide as combustion products. For liquid bath temperatures between 1065 and 1638 K, lithium and the combustion products form an immiscible liquid mixture and the denser product liquid can be removed from the combustor through a trap in order to achieve steady operation. A combustor with a maximum thermal power of 25 kW was employed to study the operation of this system, to measure performance, and to determine the properties of the immiscible liquid mixture. The experiments also examined ignition characteristics, various modes of product collection, utilization of the reactants by the combustion process, and system capabilities for long term, variable-load operation as a thermal energy source. An analysis based on the van Laar thermodynamic model was developed which satisfactorily correlates both properties and the thermal performance of the system.

Nomenclature

a_i = activity of species i
A_{ij} = empirical factor in van Laar model
b_i = empirical factor in van Laar model
f^E = excess free energy of mixing
h_i^o = standard state enthalpy of pure species i
h = mixture enthalpy
n_i = number of moles of species i
n_T = total number of moles
$\dot{m}_i$ = mass flow rate of species i
M_i = molecular weight of species i
P = pressure
$\dot{Q}_L$ = thermal power delivered to load
$\dot{Q}_P$ = parasitic power loss
Q_R = heat of reaction per unit mass of SF_6
R = universal gas constant
T = temperature
x_i = mole fraction of species i in fuel-rich liquid
y_i = mole fraction of species i in product-rich liquid
ρ_i = density of pure species i
ρ = mixture density

Introduction

POWER systems, based upon closed thermodynamic cycles and heated by closed thermal energy sources, are frequently specified for underwater applications in order to obtain operation independent of the environment. Systems of this type involving a nuclear reactor coupled to a Rankine cycle are well known for submarine propulsion. Brayton and Stirling cycles employing thermonuclear, radioisotope, energy storage, and chemical thermal energy sources have also been described.[1-6]

In the case of closed chemical thermal energy sources, volume limitations generally restrict reactant combinations to systems where the products of reaction are condensible and can be stored within a small volume, or preferably, within the volume originally occupied by the reactants. Pauliukonis[7] proposed a chemical thermal energy source which satisfies these requirements, based on the reaction between lithium and sulfur hexafluoride. Subsequent investigations have concluded that the lithium sulfur hexafluoride system is advantageous for a number of underwater applications, leading to extensive development of the concept, particularly for use with Stirling cycle engines.[1-4]

The reaction between lithium and sulfur hexafluoride yields lithium fluoride and lithium sulfide as products, according to the following stoichiometry:

$$8Li + SF_6 \rightarrow 6LiF + Li_2S$$

In work to date,[1-4] a batch reaction process has been employed for the reaction, which is illustrated schematically in Fig. 1. Prior to the start of reaction, sulfur hexafluoride is stored as a liquid in a separate tank under its own vapor pressure, while the lithium is stored as a solid within the combustion chamber. Combustion is initiated by melting the lithium and heating the liquid to conditions where reaction proceeds with gaseous SF_6, using either a solid propellant charge or electrical heaters. The vapor pressure of SF_6 is sufficiently high (22 bar at 294 K) so that gas can be drawn from the storage tank and passed directly through an injector into the combustion chamber without additional pumping.

The combustor illustrated in Fig. 1 involves submerged injection of SF_6 directly into the molten bath; combustors where reaction occurs in the combustor ullage space have also been described.[1,3] Combustion during submerged injection has been observed using X-rays for flow visualization.[8] The process can be modeled as a turbulent diffusion flame, similar to the combustion of a liquid fuel spray, except that the roles of gas and liquid are reversed for the liquid metal combustion process. Efficient combustion requires that the reaction zone be contained within the bath.

The products of reaction are liquids at typical combustor bath temperatures (1100-1300 K). Dworkin et al.[9] show that lithium and lithium fluoride form an immiscible liquid system between 1121 and 1600 K, with small quantities of lithium dissolved in the lithium fluoride phase and small quantities of lithium fluoride dissolved in the lithium phase. For combustion of lithium and SF_6, lithium fluoride is the predominant reaction product; however, lithium sulfide is also produced which dissolves in both liquid phases, changing their composition and increasing the temperature range for immiscible liquids to 1065-1638 K. Depending upon the bath-mixing generated by the injector flow, the heavier product-rich liquid can sink to the bottom of the combustor, as shown in Fig. 1, or remain as a dispersed liquid phase throughout the bath. If the bath temperature is constant, the liquid volume

Received Nov. 29, 1976; revision received Nov. 2, 1977.

Index categories: Marine Propulsion; Marine Vessel Systems, Submerged and Surface; Thermophysical Properties of Matter.

*Assistant Professor, Department of Mechanical Engineering. Presently at General Motors Research Laboratories, Warren, Mich.

†Professor, Department of Mechanical Engineering. Member AIAA.

decreases as the reaction proceeds, increasing the ullage volume within the combustor. Therefore, there is no need to remove combustion products from the system. In the absence of any inert contaminating gas within the combustor, the pressure in the ullage region is fixed by the vapor pressure of the bath and is generally below atmospheric pressure.

The energy of reaction is transferred through the bath to the cycle heat exchanger. The rate of energy release is varied by controlling the flow rate of SF_6 through the injector. Operation must be terminated when the lithium is consumed, or when low lithium concentrations require reaction volumes greater than the available volume within the combustor.

For long endurance applications, the volume required for fuel storage can become large in comparison to the volume required to complete the reaction and provide sufficient heat transfer area for the thermal load. The use of a batch combustor in this circumstance results in poor thermal response if load variations require changes in bath temperature, long start-up times, excessive parasitic heat loss and structural difficulties with large-size, high-temperature components. A steady combustor has been proposed to circumvent these difficulties.[10]

The steady lithium-sulfur hexafluoride combustor concept is illustrated in Fig. 2. The combustion chamber is sized to accommodate reaction and heat transfer requirements, while the bulk of the lithium is stored in a separate tank, to which the product liquid can also be returned if maximum volume utilization is required. Lithium is pumped to the combustor to maintain the total liquid level; the product liquid flows out of the combustor through a trap. The product liquid has a much greater density than the fuel-rich liquid. Therefore, small liquid level variations in the sump can accomodate intermittent addition of lithium, as well as ullage space pressure variations resulting from changes in bath temperature. Aside from improved response, the steady combustor provides better heat transfer characteristics since only the lithium-rich liquid, with heat transfer characteristics typical of liquid metals, is in contact with the heat exchanger throughout the operation of the system.

Previous studies of the lithium-sulfur hexafluoride combustion system have determined the relative merits of the lithium-sulfur hexafluoride reactant combination, described general hardware development, and considered some aspects of batch combustor operation.[1-4] The objective of the present investigation was to evaluate the operation and performance of the steady combustor configuration. Capabilities for restarting, idling, operation for extended periods with variable thermal load, utilization of lithium and SF_6, and thermal performance were considered. The steady combustor arrangement also facilitated measurements of parameters important to the design of both types of combustors which have not been reported previously. These include the density and composition of the bath liquids and the characteristics of the vapors in contact with the bath. A thermodynamic model is also described which correlates these measurements and provides a means of estimating bath characteristics for conditions not specifically considered during the present tests.

Steady Combustor Apparatus

The overall arrangement of the apparatus is shown schematically in Fig. 3. For experimental convenience, the test combustor had separate lithium and product storage tanks rather than the combined tank scheme. Sampling of the bath liquids was facilitated by operating the system at atmospheric pressure under argon. All components in contact with the molten bath were fabricated from type 316 stainless steel.

Combustion Chamber

The cylindrical combustion chamber had a nominal diameter of 26 cm and a length of 48 cm. The chamber was cooled by air flowing through an annular load heat exchanger designed for a maximum thermal output of 25 kW. The product-rich liquid was contained in a sump at the bottom of the combustion chamber, and was removed through a trap consisting of two coaxial tubes. The shorter inner tube extended through the bottom of the chamber, and provided a path for liquid outflow to the collection tank; the outer tube extended into a sump at the top of the chamber where crossover ports were located to vent the trap to the ullage space of the combustor in order to prevent syphoning. A sampling port which provided access to the reaction chamber was mounted on the upper sump. Both the upper and lower sumps were heated electrically to compensate for parasitic heat losses and to maintain the regions at bath temperature.

An electrical heater installed on the exterior surface of the heat exchanger was used to melt the bath prior to ignition. This start-up heater was turned off during normal operation.

Product Storage Tank

The cylindrical product storage tank had a nominal diameter of 45 cm and a length of 91 cm. The product-rich liquid leaving the combustion chamber trap entered the tank at bath temperature and was cooled by water flowing in cooling coils attached to the outside of the tank.

Lithium Supply System

The lithium storage tank was cylindrical with a nominal diameter of 27 cm and a length of 61 cm. Since the combustion chamber was filled with argon, it was convenient to transfer the fuel to the combustor with an argon lift pump mounted in the fuel tank. The lift pump required an argon flow rate 5-15% of the lithium flow rate on a mass basis. As the lithium supply was depleted, additional solid lithium was added to the tank by hand through a port at the top. The short exposure time (~ 5 s) of the fuel to ambient air prevented any detectable surface corrosion during the addition process. Electrical heaters were provided to melt the solid fuel and to maintain the liquid fuel at a temperature above 453 K.

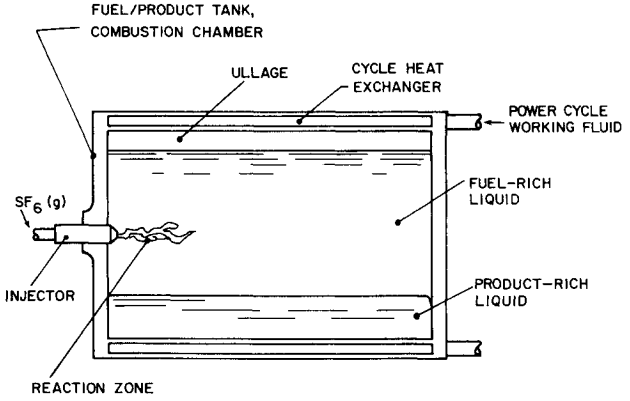

Fig. 1 Schematic diagram of the lithium-sulfurhexafluoride batch combustion process.

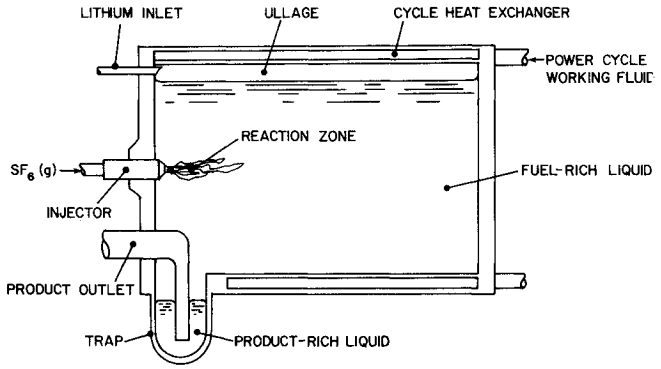

Fig. 2 Schematic diagram of the lithium-sulfurhexafluoride steady combustion process.

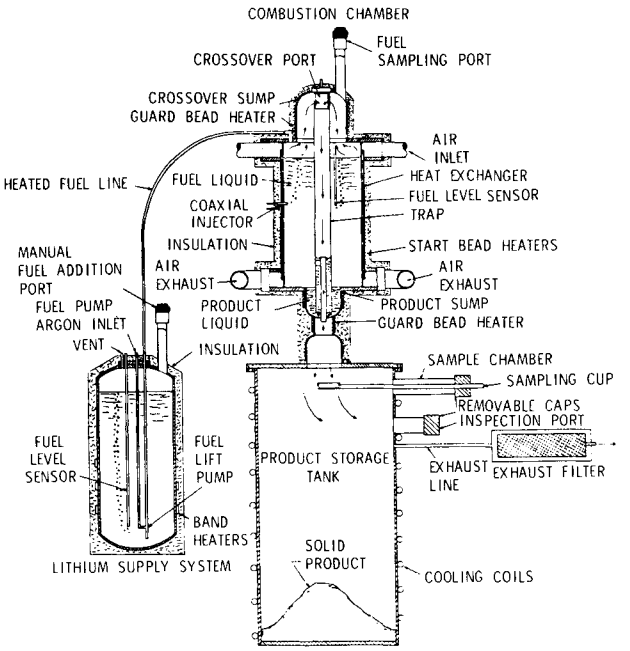

Fig. 3 Schematic diagram of the experimental air-cooled steady combustor.

The lithium was obtained from the Lithium Corporation of America having a purity of 99.9%, the major impurity being sodium.

Sulfur Hexafluoride Supply System

The SF_6 injector was mounted in the sidewall of the combustor, approximately 51 cm below the surface of the bath. The injector is shown schematically in Fig. 4. The SF_6 flowed in a small core tube fabricated from nickel 200 alloy, and was prevented from contacting the outer injector parts fabricated from type 316 stainless steel by a flow of inert argon gas in the coaxial outer tube. The SF_6 entered the argon stream near the exit of the injector. The arrangement provided reliable injector operation over the SF_6 flow range considered during the tests. Whenever the bath was molten, a purge flow of argon (0.1-0.2 kg/h) was maintained through the injector to prevent bath liquids from flowing into the lines and clogging them shut.

The SF_6 reacted in the bath, while the argon flow bubbled to the surface. All the argon flows entering the combustor passed into the product collection tank through the trap vent line. The argon was filtered after being cooled to ambient temperature to remove condensed vapors, and exhausted from the system. In a completely closed system, the argon would be recirculated back to the injector with a pump.

The SF_6 used during the tests was Matheson Gas Products certified purity grade with a listed purity of 99.8%.

Instrumentation

Temperatures were measured with chromel-alumel thermocouples recorded on null-balance, strip-chart recorders. Both the bath and the coolant air exhaust line employed four thermocouples to insure the validity of the readings.

The SF_6 and coolant airflows were controlled by pressure regulators to insure stability and measured with flow orifices. The various argon flows were measured with rotameters. Liquid levels in the combustion chamber and the lithium tank were measured with argon bubblers.

Samples of the lithium-rich liquid were withdrawn through the port at the top of the combustor using a nickel sampling cup. The sample cup could be closed by a ball mounted on a movable rod in order to prevent contamination with air. Samples of the product-rich liquid were obtained by positioning a cup below the outlet of the trap. The product sample was solidified and cooled prior to removing it from the system in order to prevent contamination. Subsequent analyses of the samples were conducted under argon in a dry box using wet chemical methods. The details of the analytical procedures are presented in Ref. 11.

Bath liquid densities were obtained by lowering an argon bubbler through the bath and measuring the pressure every 1.3 cm, obtaining readings in each phase. A linear least squares fit was made of the pressure readings in each phase; the slopes of the curves yield the two densities. These measurements were made in a radiatively-cooled steady combustor, similar to that shown in Fig. 3, but having an enlarged sump to facilitate measurements in the product-rich liquid.

Thermodynamic Model

The compostions of the two immiscible liquids present in the combustion chamber of a metal combustor are a function of bath temperature. The compositions of the corresponding fuel-rich and product-rich phases in batch and steady combustors are not the same, even at the same temperature. In batch operation, lithium sulfide and lithium fluoride are present in stoichiometric proportion within the combustor as a whole, while these proportions are only present in the product-rich liquid for steady combustor operation. A thermodynamic model for the liquids was developed which provides a means of estimating bath properties during both batch and steady operation. The model was tested by comparing predictions to steady combustor data generated during the course of this study.

The bath is a ternary immiscible mixture composed of lithium, lithium fluoride, and lithium sulfide. The mixture is nonideal as evidenced by the immiscibility characteristics of the system. Avery and Faeth[7] were able to correlate the properties of the binary mixture of lithium and lithium fluoride using a thermodynamic model for nonideal mixtures proposed by van Laar.[12] The multicomponent version of the van Laar model was used to correlate the present ternary system since lithium and lithium fluoride are the major components in the system.

To perform equilibrium calculations for a multicomponent solution, it is required that the variation of the activities of the constituent species be known as a function of temperature and composition. If a standard state is chosen as the pure component and the activity is set equal to unity in this state, then the following exact thermodynamic relationship can be derived

$$\ln\left(\frac{a_i}{x_i}\right) = \frac{1}{RT}\left(\frac{\partial[n_T f^E]}{\partial n_i}\right)_{T,P,n_j\,(j\neq i)} \tag{1}$$

The quantity f^E is the excess Gibbs free energy of mixing. For an ideal solution, f^E is zero and the activity of each species is equal to the mole fraction.

For a nonideal solution f^E is not equal to zero. For a binary solution the van Laar model yields

$$f^E = n_i n_j b_j A_{ij}/n_T(n_i b_i + n_j b_j) \tag{2}$$

where b_i, b_j, and A_{ij} are empirical parameters which are only functions of temperature and are selected to correlate binary solubility data. For a multicomponent solution, Eq. (2) can be extended[12] to yield

$$f^E = \tfrac{1}{2}\sum_i \sum_j n_i n_j b_i b_j A_{ij}/n_T \sum_i n_i b_i \tag{3}$$

where $A_{ij} = A_{ji}$ and $A_{ii} = 0$. The value of this extension is that Eq. (3) only involves parameters that can be obtained by correlating the binary data for all component pairs in the system, providing a method to predict the properties of multicomponent systems from data on the constituent binaries.

The present solution involves three binary pairs, Li-LiF, Li-Li_2S, and LiF-Li_2S, requiring the correlation of five parameters since one of the b_i parameters can be set equal to unity without loss of generality. With the correlations completed, Eq. (1) and (3) provide expressions for the activities of the various species as functions of composition and temperature. The five parameters were determined using the data of Dworkin et al.[9] for the Li-LiF binary, and data generated during this investigation for the other two binary pairs.

Denoting the mole fractions of the fuel-rich and product-rich liquid phases by x_i and y_i, equilibrium requires

$$a_i(x_i) = a_i(y_i) \qquad i = 1,2,3 \tag{4}$$

By definition the mole fractions of two phases are related as

$$\sum_{i=1}^{3} x_i = \sum_{i=1}^{3} y_i = 1 \tag{5}$$

For steady combustor operation, lithium fluoride and lithium sulfide must leave the system in stoichiometric proportions, providing a final equation

$$y_{Li_2S}/y_{LiF} = 0.1667 \tag{6}$$

Equations (4-6) provide six equations to solve for the six unknown mole fractions. The Newton-Raphson procedure was employed to solve the set of equations. The details of the calculations, the physcial property data, and the correlations for the three binary pairs are presented in Ref. 11.

The effects of nonideal mixing were also considered when thermal performance was determined. In the analysis of the system energy balance, the product-rich liquid enthalpy is given by

$$h = \sum_i x_i h_i^o + f^E - T\frac{\partial f^E}{\partial T}\bigg|_{P,n_i} \tag{7}$$

where the last two terms are the contributions from nonideal mixing.

Nonideal effects exert only a small influence on liquid densities. Therefore, density predictions were based on ideal mixing as follows

$$\rho = \sum_i M_i x_i / \sum_i (M_i x_i / \rho_i) \tag{8}$$

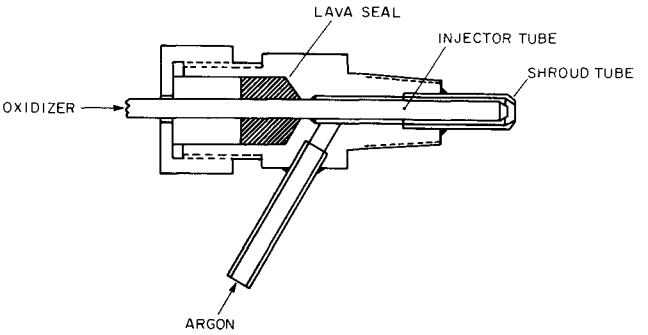

Fig. 4 Sketch of the coaxial injector.

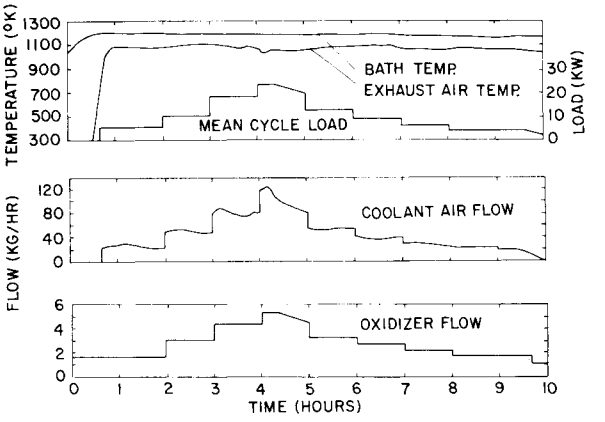

Fig. 5 Summary of run data from air-cooled combustor test No. PPC-10.

The gas phase was assumed to be an ideal mixture. In addition to Li, LiF, and Li_2S, the polymeric species Li_2, Li_2F_2, and Li_3F_3 were expected to be present in sufficient quantity to be considered in the calculations.[13] The activities of the three major species in the gas and liquid phases were equated to provide three equations to compute the composition of the gaseous mixture. Gas phase equilibrium between the major species and the polymers provided the remaining three equations required to determine the mole fractions of the six species in the gas phase. The details of this portion of the calculation may also be found in Ref. 11.

Table 1 Summary of tests with a steadily operating metal combustor

Run no.	Run length h	Oxidizer flow, kg/h	Coolant flow, kg/h	Maximum bath temp., K	Maximum power level, kW
		Radiatively-cooled combustor			
LSR-1	2.0	0.26-1.21	0.0	1264	5.75
LSR-2	1.5	0.31-1.22	0.0	1261	5.79
LSR-3	7.1	0.14-0.88	0.0	1233	4.18
LSR-4	1.3	0.32-0.88	0.0	1177	4.18
LSR-5	7.1	0.0 -0.95	0.0	1272	4.51
LSR-6	5.6	0.0 -2.25	0.0	1219	10.7
LSR-7	3.2	0.0 -0.83	0.0	1297	3.94
LSR-8	4.5	0.0 -2.77	0.0	1252	13.2
		Air-cooled combustor			
PPC-1	2.4	2.26	22.0-84.9	1208	10.8
PPC-2	2.6	0.90-2.27	31.8-43.0	1213	10.8
PPC-3	1.4	2.27	20.1-48.8	1225	10.8
PPC-4	3.8	0.75-2.25	0.0	1210	10.7
PPC-5	2.5	0.75-1.88	16.4-37.7	1172	8.9
PPC-6	0.9	0.76	0.0	1161	3.6
PPC-7	2.8	0.56-1.13	0.0	1238	5.4
PPC-8	5.2	0.47-1.13	0.0	1255	5.4
PPC-9	6.3	1.31-4.96	18.0-109.	1205	23.6
PPC-10	10.0	1.11-5.29	11.0-127.	1205	25.2

Results and Discussion

Ignition and Start-up

In the case of quiescent molten lithium surfaces in contact with SF_6, Little[14] found that combustion would only proceed at temperatures greater than 1065 K, the melting temperature of the product liquid, and suggested that the solid product protects the surface. In the present tests, however, the submerged injector agitates the liquid, creating a fresh surface and making it possible to ignite the reaction by starting the oxidizer flow at any temperature above the melting point of lithium (453 K).

Product-rich liquid outflow does not occur during the early stages of heat-up, since the product contained in the sump is solid and excess product accumulates within the combustor, similar to a batch process. When the sump and trap melt out, the excess product flows out of the system. The bath level can then be brought up to the operating condition by adding lithium. When the bath reaches the desired operating temperature, the flow can be intermittently controlled by the liquid level in the bath, as noted earlier.

Oxidizer Utilization

An auxiliary apparatus was used to determine the quantity of unreacted SF_6 carried from the bath with the argon flow. The gas composition was determined using a gas chromatograph which could detect SF_6 concentrations in argon as small as 10 ppm. During start-up conditions, at temperatures below 870 K, small quantities of SF_6 were detected yielding SF_6 consumption as low as 99.5%. At higher temperatures, reaction was complete and no SF_6 could be detected in the argon flow leaving the combustor.

System Operation

A summary of the tests conducted with both the radiative and air-cooled steady combustors is presented in Table 1. The radiative combustor tests were conducted to develop various aspects of the system prior to the design of the air-cooled system and to measure bath liquid densities. Tests with the air-cooled combustor provided the bath composition and thermal performance data. During the test program, combustors were routinely restarted after weeks of storage at ambient temperature. Combustors were operated at variable thermal power with temperatures as high as 1297 K and test times as long as 10h. Bath temperatures were limited to 1297 K by material considerations, primarily material strength.

Typical test results are illustrated in Fig. 5 where SF_6 flow, coolant airflow, bath temperature, exhaust air temperature, and thermal power output are given as a function of time. The thermal load was varied by changing the coolant flow rate and adjusting the oxidizer flow accordingly. During this test, power level was first increased and then decreased in steps while maintaining a relatively constant bath temperature of 1197 ± 3 K. However, arbitrary power level changes over the load range, as well as bath temperature changes, were also possible. Temperatures were very uniform in the fuel-rich portion of the bath, due to the good heat transfer characteristics of the molten metal. The maximum temperature variation measured in this phase was less than 1 K at full power conditions. The temperature effectiveness of the heat exchanger was 88% at design power levels; therefore, the exhaust air temperature remained relatively constant as the thermal load varied. A total of 26.4 kg of SF_6 and 10.0 kg of lithium were consumed during the test described in Fig. 5.

Product Collection

The reaction products produced during the radiative and air-cooled combustor tests were collected in a tank originally empty at the start of a test. Figure 6 is a photograph of the reaction products collected during air-cooled combustor test 9, and is typical of products collected during all tests. The products developed a stalagmite formation extending from the bottom of the collection tank, which grew in width as the test proceeded once its upper end neared the outlet of the trap. The formation did not adhere to the collection tank and could be easily removed.

The more compact arrangement which involves returning the products to the lithium storage tank was also investigated. At atmospheric pressure, the product-rich liquid was exhausted into molten lithium at a temperature of 505 K. The temperature of the product-rich liquid flowing from the trap was 1227 K, with flow rates in the range 3.5-5.5 kg/h. Figure 7 is a photograph of a typical sample of a product collected in this manner. The product solidified into irregular balls with maximum dimensions ranging up to 1 cm in diameter. The packing efficiency of the balls was approximately 50% on a

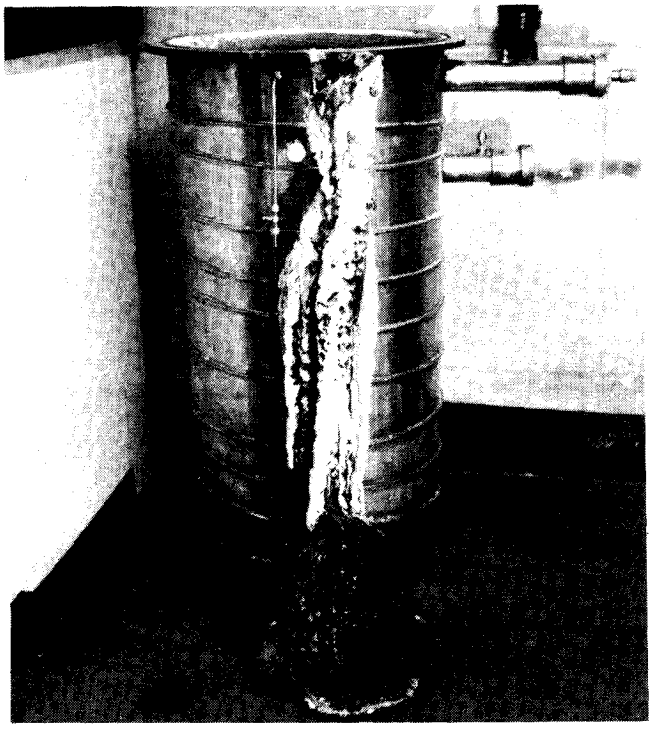

Fig. 6 Photograph of reaction products.

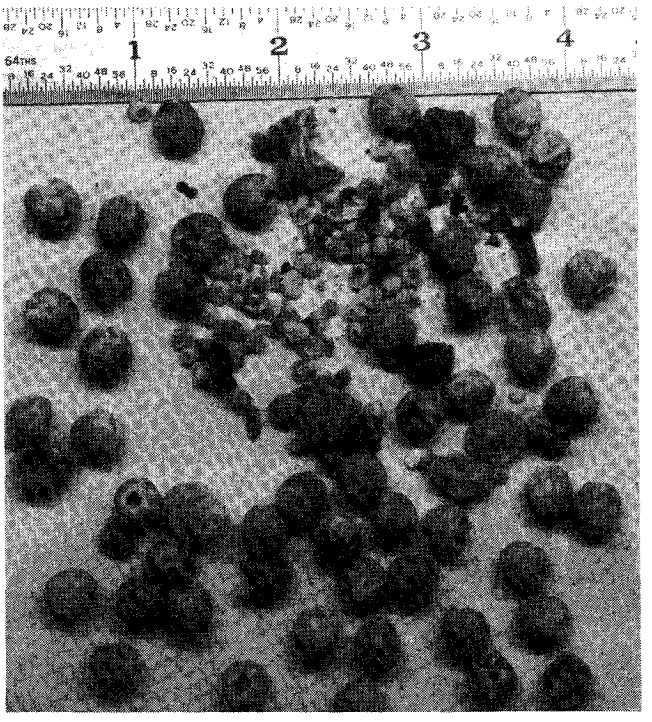

Fig. 7 Photograph of wet-tank reaction products.

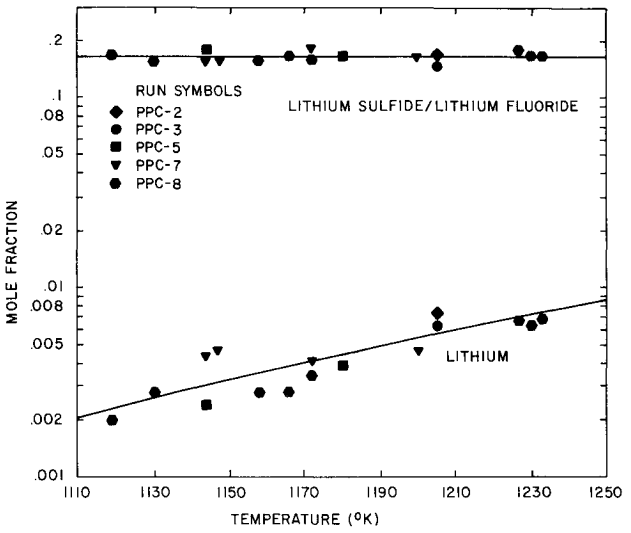

Fig. 8 Composition of the product-rich liquid.

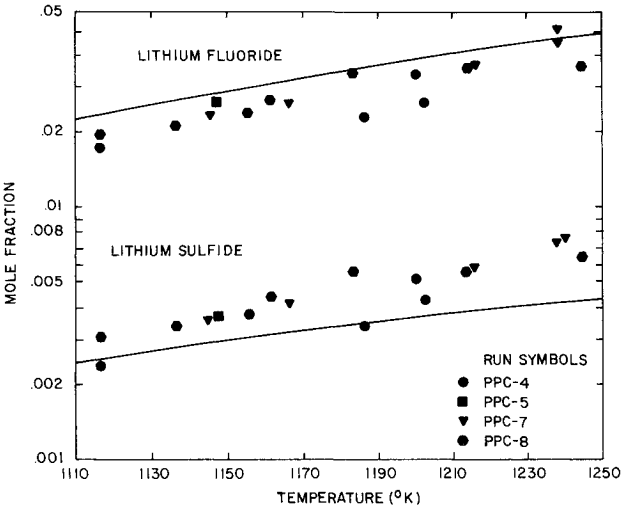

Fig. 9 Composition of the fuel-rich liquid.

volume basis. The material appeared to have solidified smoothly without shattering, possibly because the temperature of the product was below the boiling point of lithium at atmospheric pressure.

Bath Liquid Composition

Figures 8 and 9 compare measurements of the composition of the bath liquids at various temperatures with the predictions of the van Laar model. Repeatability of the measurements for different tests was reasonably good with the model in fair agreement with the data.

The product-rich liquid phase results in Fig. 8 are presented as the mole fraction of lithium and the ratio of the mole fraction of lithium sulfide to the mole fraction of lithium fluoride. The ratio of the concentrations of the product species is in good agreement with the stoichiometry specified by Eq. (6), indicating that steady operation was achieved. The concentration of lithium in the product-rich liquid increases with temperature, but is relatively low over the temperature range of these tests – less than 0.9% on a molar basis. This suggests good fuel utilization for a steady combustor, even if lithium is trapped within the product as it solidifies.

Results for the fuel-rich liquid phase are presented in Fig. 9 as the mole fraction of lithium fluoride and lithium sulfide as a function of temperature. The remainder of the phase is lithium. The concentrations of lithium fluoride and lithium sulfide increase with temperature; however, the lithium concentration is greater than 95% on a molar basis over the temperature range of the tests. The high concentration of molten metal in this portion of the bath accounts for its good heat transfer characteristics.

Bath Liquid Densities

Bath liquid densities at various temperatures are compared with predictions of the thermodynamic model in Fig. 10. The density of the fuel-rich phase is relatively constant, because as the temperature increases the reduced density of the components is balanced by the increased concentration of the denser product species. Reduced component densitites and increased lithium concentrations both act to reduce the density of the product-rich liquid as the temperature increases.

The ratio of the density of the product-rich liquid to the lithium-rich liquid is 3.2-3.4 in the temperature range of the measurements. As noted earlier, this large ratio is desirable for flexible steady combustor operation, since intermittent lithium addition to the system can be accommodated by small changes in the level of the product liquid.

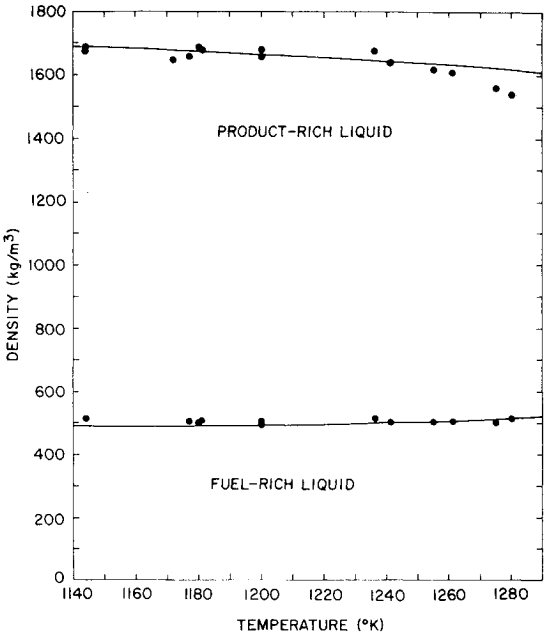

Fig. 10 Density of the bath liquids.

Bath Vapor Pressure

Vapor pressures could not be measured accurately in the apparatus illustrated in Fig. 3, due to the presence of microdroplets formed as the argon flow disengaged from the bath liquid. Therefore, these measurements were made in an apparatus where no argon flow was present, allowing direct determination of the total vapor pressure of the bath under conditions representative of steady combustor operation.[11]

Figure 11 illustrates the comparison between measured and predicted total vapor pressures at various bath temperatures. The calculations indicate that Li and Li_2 are predominant species in the vapor phase, comprising over 99% of the mixture on a molar basis.

Thermal Performance

Thermal performance was determined by measuring the thermal power transferrred to the load at various SF_6 flow rates for a fixed bath temperature of 1197 ± 3 K. During these measurements, the temperature of the lithium entering the combustor was fixed at 533 K and the oxidizer at 305 K. The thermal power was determined as the product of the flow rate and enthalpy rise of the air coolant, with the enthalpy rise

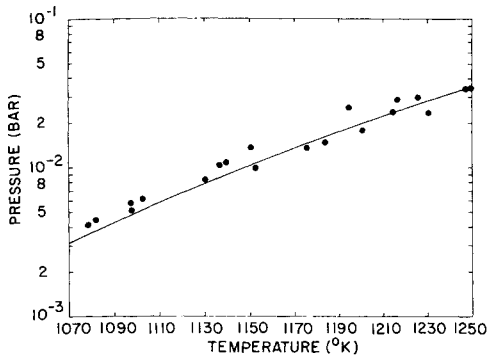

Fig. 11 Total vapor pressure of the bath liquids.

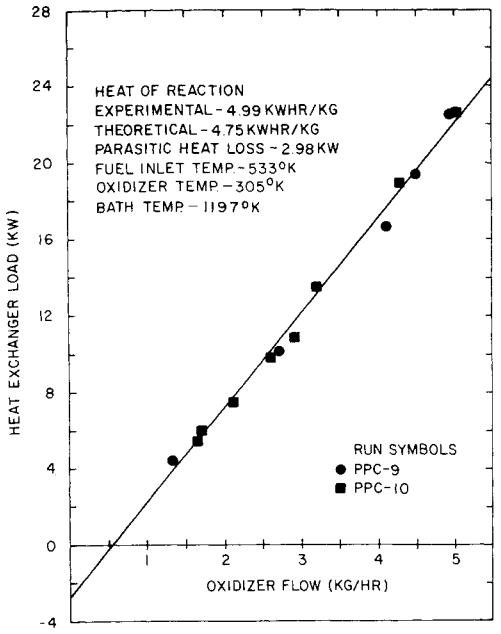

Fig. 12 Thermal performance test data.

determined from the air temperature change using tabulated enthalpies.

The results are plotted in Fig. 12 for the two tests where thermal performance was evaluated. The repeatability of the measurements is seen to be good. Under steady conditions, for constant bath and reactant temperatures, the chemical energy released per unit mass of SF_6 is a constant given by

$$\dot{m}_{SF_6} Q_R = (\dot{m}h)_{SF_6 \text{inlet}} + (\dot{m}h)_{Li\ \text{inlet}} - (\dot{m}h)_{\text{Prod. outlet}} \quad (9)$$

The combustor energy balance is

$$\dot{m}_{SF_6} Q_R = \dot{Q}_L + \dot{Q}_P \quad (10)$$

where $\dot{Q}_L$ is the thermal power delivered to the load and $\dot{Q}_p$ the parasitic heat loss. The variation of SF_6 flow rate with thermal load is nearly linear, as indicated by the least squares line passed through the data in Fig. 12. Under these circumstances, Eq. (10) indicates that the parasitic heat loss is nearly constant and Q_R can be determined as the slope of this line, yielding an energy release rate of 4.99 kW-h/kg of SF_6 for these operating conditions. For the same conditions, the thermodynamic model predicts an energy release rate of 4.75 kW-h/kg of SF_6. The 5% discrepancy between the two measurements is compatible with the experimental accuracy of the thermal load evaluation, the effect of some variation in parasitic heat loss with load, and uncertainties in the physcial properties of the bath materials. The average parasitic heat loss of the system is given by the negative intercept on the load

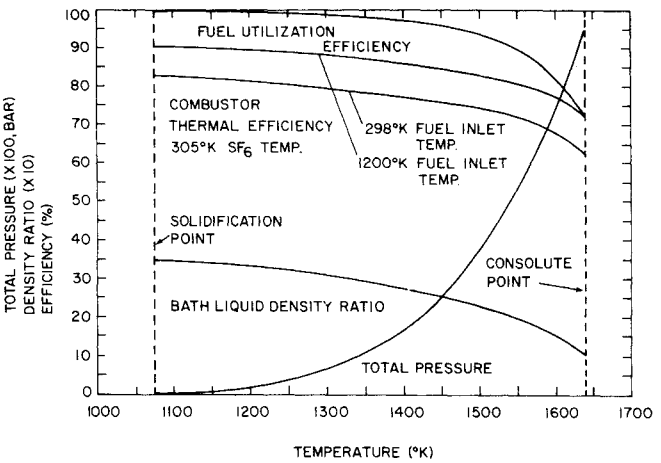

Fig. 13 Effect of bath temperature on system performance.

axis and was found to be equal to 2.98 kW for this combustor arrangement at a bath temperature of 1197 K. The parasitic heat loss would increase slightly with increasing bath temperature.

Bath Temperature Effects

The thermal efficiency of closed cycle powerplants increases as the temperature of the working fluid leaving the thermal energy source is increased. This implies higher bath temperatures for the lithium-sulfur hexafluoride combustor, which can lead to poorer thermal performance of the combustor unless special provisions are made to usefully recover the energy carried from the combustor by the molten reaction products.

Since the thermodynamic model gave reasonable predictions of bath properties and thermal performance, calculations with the model were extended to examine the effects of bath temperature during steady combustor operation. The results are summarized in Fig. 13 for the bath temperature range between the product solidification temperature, 1065 K, and the temperature where the two liquid phases become miscible, 1638 K. This represents the temperature range where operation of a trapped steady combustor is possible.

The fuel utilization efficiency plotted on Fig. 13 is the fraction of the lithium flow that is reacted in the combustor. The parameter decreases as the bath temperature increases since the increased solubility of lithium in the product-rich liquid at high temperatures results in increased amounts of lithium being carried from the combustor along with the products. A portion of this dissolved lithium might be recovered as the products cool, if the products are returned to the lithium storage tank.

The combustor thermal efficiency represents the percentage of the standard heat of reaction at 298 K, 5.65 kW-h/kg of SF_6, which is transferred to the load at a given bath temperature in the absence of parasitic heat losses. Parasitic losses are not included, as they are strongly dependent on combustor configuration and can be utilized in some applications. The two curves shown on Fig. 13 are for two different lithium inlet temperatures, and were calculated assuming that the energy used to preheat the fuel was reclaimed from the product liquid. Energy can be reclaimed from the product liquid by returning the liquid to the lithium storage tank. The thermal efficiency is based on the SF_6 flow since this reactant is completely consumed during combustion. The thermal efficiency based on the lithium flow is lower, comprising the product of the fuel utilization efficiency and the thermal efficiency based on the SF_6 flow, if lithium in the product-rich liquid is not recovered. For the case where solid lithium at 298 K enters the combustor, the thermal efficiency based on SF_6 flow decreases from 83% at the

product solidification temperature to 62% at the consolute temperature. The corresponding values for the case where liquid lithium enters the combustor at 1200 K are 91% at the solidification point and 73% at the consolute point. The overall thermal efficiency of the combustor system can be increased above these values if additional energy is recovered from the products during cooling and is used for other applications within the vehicle.

Other operating parameters illustrated in Fig. 13 include the bath liquid density ratio and the mixture vapor pressure. The bath liquid density ratio is the ratio of the product-rich liquid density to the fuel-rich liquid density, decreasing from 3.53 at the solidification temperature to unity at the consolute temperature. The vapor pressure of the bath increases rapidly as the temperature is increased, reaching 0.95 bar at the consolute temperature.

Summary and Conclusions

The characteristics of a closed thermal energy source based on the steady combustion of sulfur hexafluoride and molten lithium were investigated. The system was operated at bath temperatures of 1110-1297 K, with arbitrary thermal load variations in the range 0-25 kW. Single periods of operation extended up to 10 h. The system could be restarted as desired after extended periods of storage at room temperature by introducing SF_6 through a submerged injector at any temperature above the melting point of lithium. For bath temperatures above 870 K and injector submergence depths greater than 10 cm, reaction of SF_6 was complete.

For conditions of steady combustor operation, measurements were made of bath composition, density, vapor pressure, and thermal performance. A thermodynamic analysis, based on the van Laar model for the properties of nonideal liquid mixtures,[12] was found to provide an adequate correlation of the measurements. The availability of this model provides a means of estimating bath liquid properties in cases where composition boundary conditions differ from steady combustor operation.

Operation of a trapped steady combustor with the present reactants is theoretically possible between 1065 and 1638 K, however, combustor performance declines as the bath temperature is increased. For bath temperatures less than 1250 K:

1) Less than 1% on a molar basis of the lithium is carried out of the bath with the products.

2) More than 83% of the standard heat of reaction at 298 K can be transferred to the load, exclusive of parasitic heat losses.

3) The lithium-rich portion of the bath has a molar concentration of lithium greater than 95%. The predominance of liquid metal in this portion of the bath produces relatively uniform bath temperatures and good heat transfer characteristics.

Test durations during the present investigation were relatively short in comparison to the endurance objectives of long-term thermal energy sources. However, indications of corrosion or deterioration of the combustor that would prohibit longer periods of operation were not encountered during the present tests.

Acknowledgment

This work was supported by the David W. Taylor Naval Ship Research and Development Center, Annapolis Laboratory, as Technical Agent for the Defense Advanced Research Projects Agency.

References

[1] Mattavi, J. N., Heffner, F. E., and Miklos, A. A., "The Stirling Engine for Underwater Vehicle Applications," SAE National Powerplant Meeting, Paper 690731, Oct. 27-29, 1969.

[2] van der Slujis, W.L.N., "A Lithium/Sodium/Sulfur-hexafluoride Heat Source in Combination with a Stirling Engine as a Propulsion System for Small Submersibles," *Proceedings of Tenth Intersociety Energy Conversion Engineering Conference*, 1975, pp. 1031-1037.

[3] Uhlemann, H., Spigt, C. L., and Hermans, M. L., "The Combination of a Stirling Engine with a Remotely Placed Heat Source," *Proceedings of Ninth Intersociety Energy Conversion Engineering Conference,* 1974, pp. 620-629.

[4] Biermann, U. K. P., "The Lithium/Sulfurhexafluoride Heat Source in Combination with a Stirling Engine as an Environmental Independent Underwater Propulsion System," *Proceedings of Tenth Intersociety Energy Conversion Engineering Conference,* 1975, pp. 1023-1030.

[5] DeVries, G., Karig, H. E., and Drage, G., "Eutectic Molten Salt Thermal Energy Storage System," *Journal of Hydronautics*, Vol. 3, Oct. 1969, pp. 191-195.

[6] Phillips, T. W., "Closed Cycle Turbine as a Proposed Undersea Power Source," *Journal of Hydronautics*, Vol. 3, Oct. 1969, pp. 184-190.

[7] Pauliukonis, R. S., "Fuel System Comprising Sulfur Hexafluoride and Lithium Containing Fuel," U. S. Patent 3,325,318, June 13, 1967.

[8] Avery, J. F. and Faeth, G. M., "Combustion of a Submerged Gaseous Oxidizer Jet in a Liquid Metal," Fifteenth International Symposium on Combustion, The Combustion Institute, 1974, pp. 501-512.

[9] Dworkin, A. S., Bronstein, H. R., and Bredig, M. A., "Miscibility of Metals and Salts. VI. Lithium-Lithium Halide Systems," *Journal of Physical Chemistry*, Vol. 66, 1962, pp. 572-573.

[10] Faeth, G. M., "Steady Heat Generating Reactor," U.S. Patent 3,838,658, Oct. 1, 1974.

[11] Groff, E. G., "Characteristics of a Steadily Operating Metal Combustor," Doctoral Dissertation, Mechanical Engineering Dept., Pennsylvania State Univ., Aug. 1976.

[12] Wohl, K., "Thermodynamic Evaluation of Binary and Ternary Liquid Systems," *Transactions of the American Institute of Chemical Engineers,* Vol. 42, 1946, pp. 215-249.

[13] Berkowitz, J. and Chupka, W. A., "Composition of Vapors in Equilibrium with Salts at High Temperatures," *Annals of the New York Academy of Sciences,* Vol. 79, 1960, pp. 1073-1078.

[14] Little, T. E., "Reactivity of Nitrogen, Oxygen, and Halogenated Gases with Molten Lithium Metal," Doctoral Dissertation, Mechanical Engineering Dept., Pennsylvania State Univ., 1973.